ELSEVIER

Surface Science 328 (1995) 159–169

surface science

Studies of $LaAlO_3\{100\}$ surfaces using RHEED and REM II: 5×5 surface reconstruction

Z.L. Wang *, A.J. Shapiro

National Institute of Standards and Technology, Bldg. 223, Gaithersburg, MD 20899, USA

Received 27 September 1994; accepted for publication 2 December 1994

Abstract

For the first time, 5×5 surface reconstruction on annealed $LaAlO_3\{100\}$ surfaces is observed with reflection high-energy electron diffraction (RHEED) and reflection electron microscopy (REM). Most of the {100} surface areas are covered by the reconstructed layer. The presence of twin boundaries and protrusion contaminants on the surface has no influence on the formation of the reconstruction. Surface steps may enhance the surface reconstruction but are not essential to initiate the reconstruction. This feature is interpreted based on the adsorption models of oxygen on surface steps.

Keywords: Lanthanum-aluminate; Reflection electron microscopy (REM); Stepped single crystal surfaces; Surface structure, morphology, roughness, and topography

1. Introduction

In our previous paper on the surface structures of $LaAlO_3\{100\}$ [1], hereafter referred to as Paper I, surface step structures, dislocation and twin boundaries have been studied in detail. The reconstruction of $LaAlO_3\{100\}$ was also noticed in the patterns of reflection high-energy electron diffraction (RHEED). As illustrated in Paper I, $LaAlO_3\{100\}$ is an optimum substrate for the growth of high-temperature superconductor $YBa_2Cu_3O_{7-x}$ thin films. The reconstruction of surface atoms may critically affect the nucleation and growth of epitaxial films on $LaAlO_3\{100\}$ substrates, because the reconstructed surface may not preserve the smallest mismatch between the substrate and $YBa_2Cu_3O_{7-x}$ films. Thus the growth direction and quality of the films may be greatly affected. In this paper, we present our detailed studies of the 5×5 reconstruction on $LaAlO_3\{100\}$. RHEED and reflection electron microscopy (REM) are combined to define the surface reconstruction. Relationships between surface reconstruction and the distribution of surface steps and {100} twin boundaries will be illustrated.

2. Experimental results and analysis

For REM observations, bulk specimens were prepared by cutting $LaAlO_3$ single crystal sheets into pieces with dimensions of about $2.5 \times 1 \times 0.8$ mm. The (100) surface was mechanically polished before annealing. The polished surface was annealed at 1500°C for 20 h in air. REM images were recorded

* Corresponding author. Present address: School of Materials Science and Engineering, Georgia Institute of Technology, Atlanta, GA 30332-0245, USA. Fax: +1 404 853 9140. E-mail: zwang@enh.nist.gov.

SSDI 0039-6028(95)00015-1

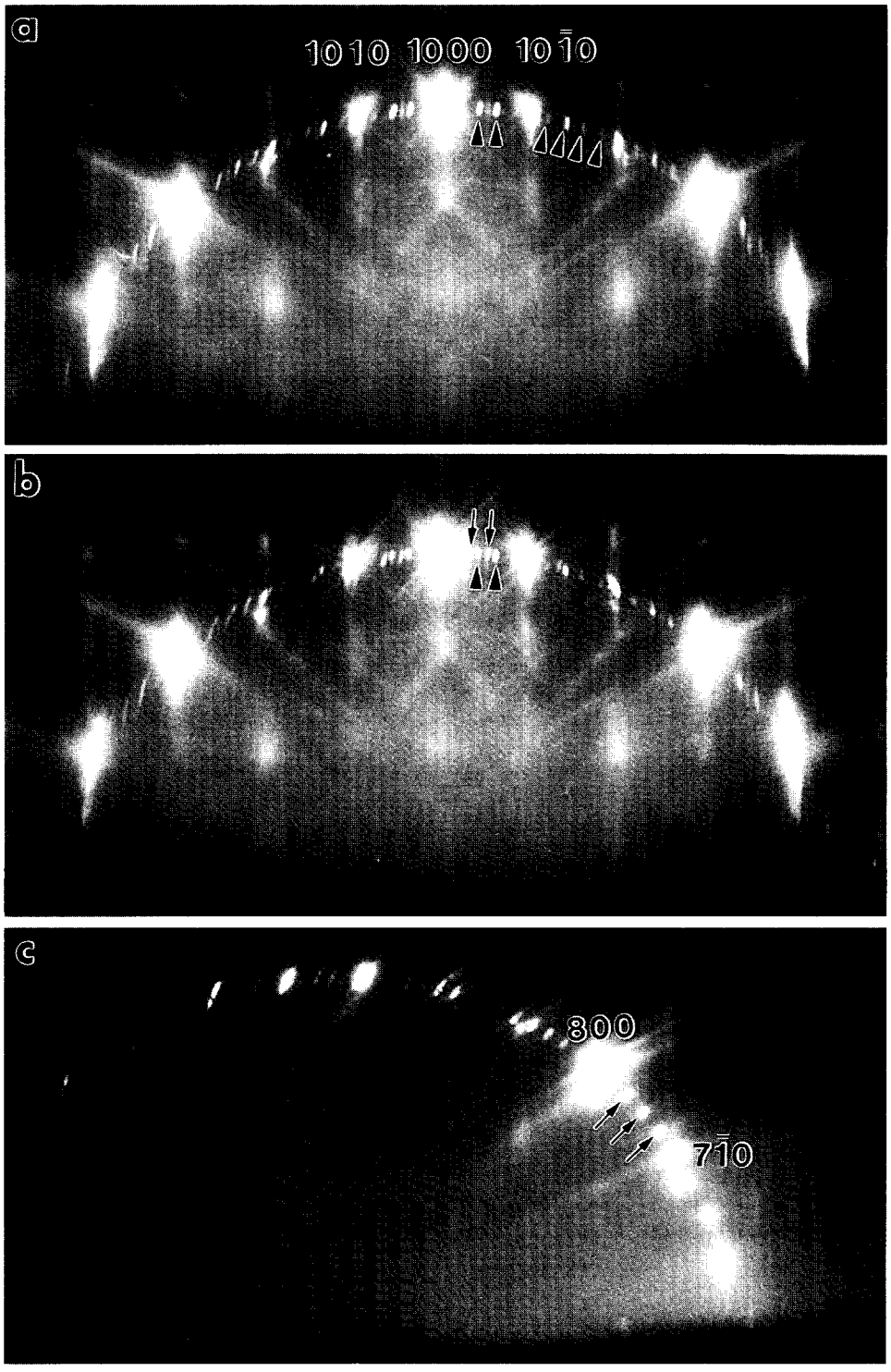

Fig. 1. RHEED patterns recorded from an annealed $LaAlO_3(100)$ surface showing the reconstruction of the surface top atomic layer. The double splitting of the superlattice reflections in (b) have resulted from the twin structure of the crystal (see text). (c) RHEED pattern recorded when the specimen is tilted to show the reconstruction along the direction perpendicular to the beam.

with Philips EM430 (300 kV) and Philips EM400T (120 kV) TEMs. The high-resolution REM (HR-REM) images were taken at 300 kV with the Philips EM430. Detailed experimental method and instruments have been introduced in Paper I.

$LaAlO_3$ is a face-centered rhombohedral structure [2]. The structure is that of distorted-perovskite with lattice constant $a = 0.3788$ nm and $\alpha = 90.066°$. In the structure unit cell, the La^{3+} ion locates at (000), the Al^{3+} ion at $(\frac{1}{2}\frac{1}{2}\frac{1}{2})$, and the O^{2-} ions at the face-centers $\{\frac{1}{2}\frac{1}{2}0\}$. {100} twin planes are frequently seen, which are formed during the phase transformation of $LaAlO_3$ [3].

In this section, we first present experimental results to identify the surface reconstruction. Then we will illustrate the relationship between the observed surface reconstruction and the surface defects and steps.

2.1. 5×5 surface reconstruction

Fig. 1 shows a group of RHEED patterns recorded from an annealed $LaAlO_3(100)$ surface when the incident beam strikes the surface near the [001] azimuth. In Fig. 1a, two strong superlattice reflections are seen between bulk reflections (1000) and (10 $\bar{1}$ 0). The two superlattice reflections are separated by $\frac{1}{5}(0\bar{2}0)$ and $\frac{1}{5}(020)$, respectively, from the

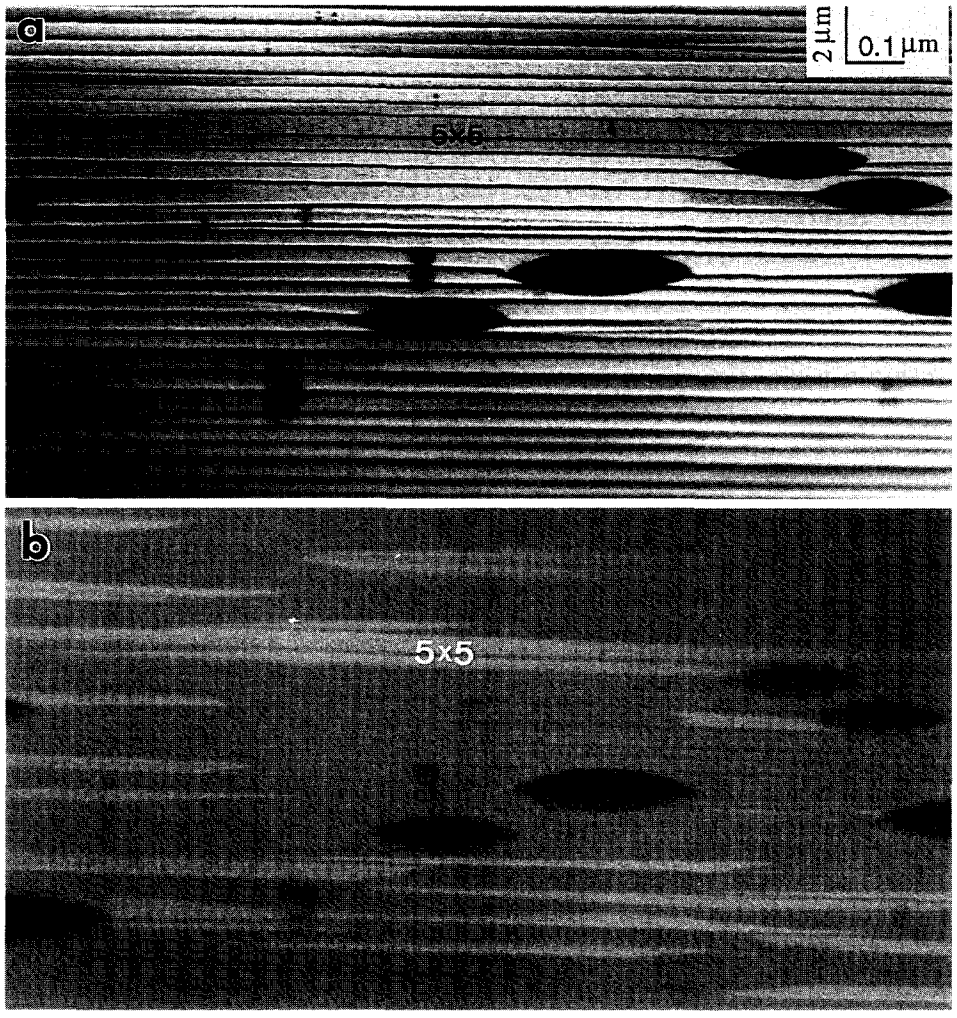

Fig. 2. REM images recorded using (a) the (10 0 0) specularly reflected beam and (b) the superlattice reflections, showing the distribution of 5×5 reconstruction on the (100) surface.

(1000) and (10 $\bar{1}$ 0) bulk reflections. On the right-hand side of (10 $\bar{1}$ 0) reflection, four equally-spaced superlattice reflections are seen.

In Fig. 1a, a weak reflection located half-way between the two superlattice reflections is seen. In order to find the origin of this reflection, the following study was performed. As presented in Paper I, {100} twin structures are observed in $LaAlO_3$, which can cause a double splitting of the Bragg reflected spots. We now slightly change the illumination area and increase the convergence of the incident beam, so that the diffractions from the twin grains are equally seen in the pattern, as shown in Fig. 1b, where the superlattice reflections are doubled in comparison to those shown between the (1000) and (10 $\bar{1}$ 0) bulk reflections. The matrix reflections, such as (1000) and (10 $\bar{1}$ 0), are also doubled, but the doubling is not seen in the displayed pattern due to their overexposure. This pattern is consistent with the conclusion that the weak spot seen between the two superlattice reflections in Fig. 1a came from the surface diffraction of one of the twined grains which was not strongly excited.

To see the equivalent excitation of the superlattice reflection along [010], a direction parallel to the (100) surface, the crystal was slightly rotated and the

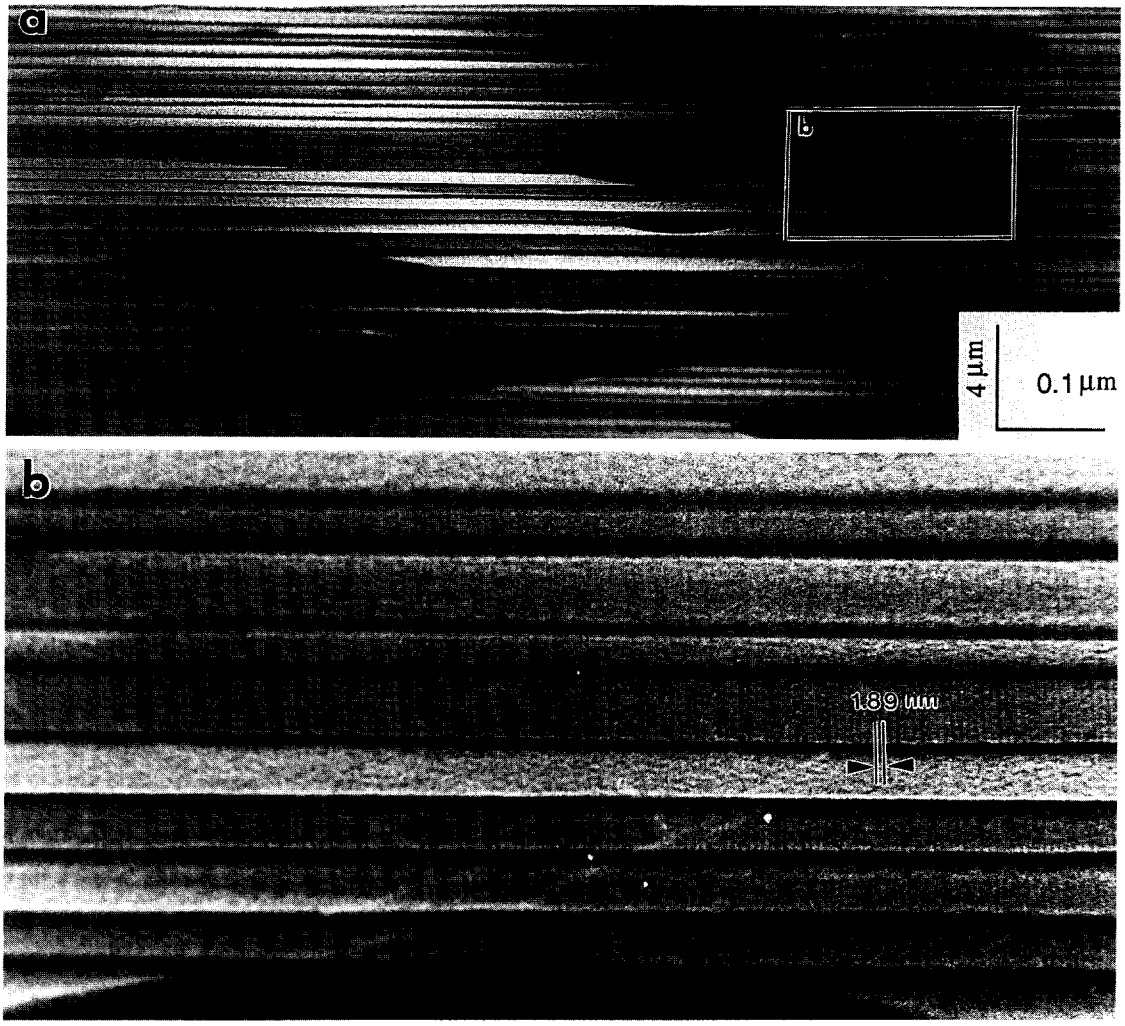

Fig. 3. High-resolution REM images of the $LaAlO_3$(100) surface, showing the interference fringes between (10 0 0) and the superlattice reflected beams; (b) is an enlargement of the area b indicated in (a).

corresponding pattern is shown in Fig. 1c. Three superlattice reflections are clearly seen. The superlattice reflection next to the (800) reflection is shadowed by the brightness of the (800) beam. The superlattice reflection next to the $(7\bar{1}0)$ is seen.

Therefore, as a summary of Fig. 1, superlattice

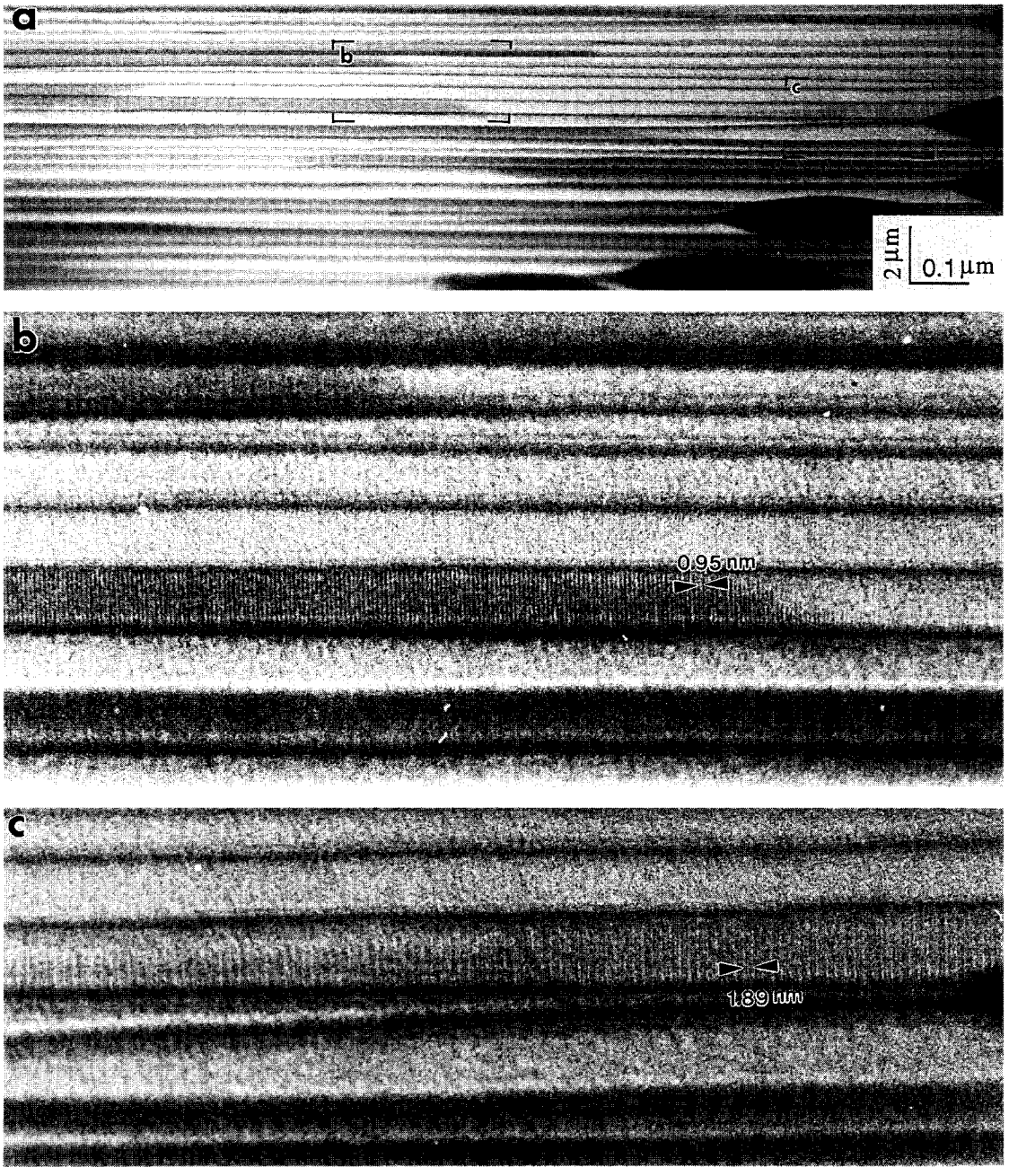

Fig. 4. High-resolution REM images of the $LaAlO_3(100)$ surface, showing the interference fringes between (10 0 0) and the superlattice reflected beams; (b) and (c) are the enlargements of the areas b and c indicated in (a), respectively.

reflections equally separated by $\frac{1}{5}(0\bar{1}0)$ of $LaAlO_3$ are seen. The patterns, however, can be interpreted by either of the following two possible structures: (1) 5×5 surface reconstruction, or (2) a second phase which has a supercell that is five times the cell for $LaAlO_3$. An example in correspondence to case (2) has been observed on MgO{100}, which displayed the "4×4" superlattice reflections when annealed to 1200°C in situ, and the superlattice reflections were due to the formation of the MgO_2 phase on the surface [4].

To determine which structure we have seen, REM images are recorded using the (10 0 0) specular reflection and the two superlattice reflections distributed between (10 0 0) and (10 $\bar{1}$ 0), and the results are shown in Figs. 2a and 2b, respectively. In the image recorded using (10 0 0) (Fig. 2a), the surface shows brighter and darker contrast regions. In the image recorded with the superlattice reflections (Fig. 2b), the contrast is reversed in comparison to Fig. 2a. In Figs. 2a and 2b, the contrast is complementary. The surface is rather smooth and there is no surface roughness in the areas which produce the superlattice reflections. Based on the previous studies of MgO(100) [4], the surface morphology would be rough if there were a second phase being formed on the surface, Therefore, the $LaAlO_3$(100) surface exhibits the 5×5 reconstruction. The reconstructed surface areas show darker contrast in the REM image recorded using the (10 0 0) reflection because of the reduction of the (10 0 0) reflected intensity due to the simultaneous excitation of the superlattice reflections.

The dark particles, which were found to be Si–La–O in Paper I, are "randomly" distributed on the surface, and they do not show any preference to distribute on either the 5×5 reconstructed (bright contrast areas in Fig. 2b) or the unreconstructed (dark contrast areas in Fig. 2b) surface regions. Microanalysis with energy dispersive X-ray spectroscopy with a scanning electron microscopy shows that the Si content is below the detection limit, which is typically about 1%–2%. Thus, the surface reconstruction appears to be uncorrelated with the presence of Si–La–O particles.

In order to confirm the existence of the 5×5 reconstruction, HR-REM images are recorded by selecting the (10 0 0) and superlattice reflected beams using a larger objective aperture, and the corresponding image is shown in Fig. 3a. Structures analogous to those shown in Fig. 2a are seen. Fig. 3b is an enlargement of the area b indicated in Fig. 3a. Two characteristics are seen. First, the reconstructed surface areas exhibit fringes, which are equally spaced with a separation of 1.89 nm. The unreconstructed regions are in brighter contrast and do not display fringes. The fringes can only be seen in the near focus region due to the smaller depth of focus for a larger objective aperture.

Fig. 4 shows another group of HR-REM images of the (100) surface. These images share the same characteristics as those seen in Fig. 3. Figs. 4b and 4c are enlargements of the areas b and c, respectively, indicated in Fig. 4a. Fringes separated by 0.95 nm are seen in Fig. 4b. The 1.89 nm fringes observed in Fig. 4c are the same type of structure as seen in Fig. 3b. It is apparent that the contrast of the 0.95 nm spaced fringes is better than that of the 1.89 nm spaced fringes.

The HR-REM images shown in Figs. 3 and 4 have confirmed the existence of the 5×5 reconstruction on the annealed $LaAlO_3$\{100\} surfaces. The fringes are the interference of the superlattice reflections with the (10 0 0) beam, as interpreted in the following.

To understand the spacing of the fringes seen in Figs. 3 and 4, Fig. 5 shows a schematic of the reflected beams observed near the (10 0 0) reflection as shown in Fig. 1a. There are four superlattice reflections between (10 0 0) and (10 $\bar{1}$ 0), as indicated with S_1 to S_4. In correspondence to S_1 to S_4, S_1' to S_4' are the symmetric spots on the left-hand side of (10 0 0). S_2 and S_3 are the two strong superlattice reflections indicated by arrowheads in

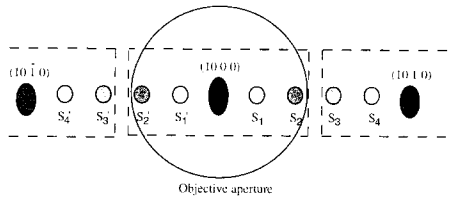

Fig. 5. A schematic diagram showing the distribution of superlattice reflections near the bulk reflections in reference to Fig. 1a. The darkness of the spot qualitatively indicates the intensity of the reflected beam.

Fig. 1a. S_1 and S_4 are two weak reflections. The circle indicates the objective aperture used for HR-REM imaging. Since S_1 is separated by $\frac{1}{5}(0\bar{1}0)$ from (10 0 0), the interference of the two produces fringes with equal spacing of $5a = 1.89$ nm, in agreement with the experimental observations shown in Figs. 3 and 4. The interference between S_2 and (10 0 0) gives fringes with separation which is half of that produced between S_1 and (10 0 0), thus exhibiting the 0.95 nm fringes seen in Fig. 4. Therefore, S_1 and S_2 are generated from the rescattering of the (10 0 0) beam. Similarly, S_3 and S_4 are generated from the rescattering of the (10 $\bar{1}$ 0) beam. Thus, S_4 is equivalent to S_1, both showing weak intensity; and S_3 is equivalent to S_2, both showing strong intensity. The weak intensity of S_1 in comparison to that of S_2 results in the poorer contrast of the 1.89 nm fringes than that of the 0.95 nm fringes, as observed in Figs. 4b and 4c.

The weak intensity of S_1 in comparison to that of S_2 may give us a hint about the types of units which compose the supercell of 5×5 reconstruction. S_1 is weak but is not forbidden. Thus, there are probably two types of units in the supercell, giving reflections that are out of phase for the S_1 beam and are in phase for the S_2 beam. Determination of the distribution and symmetry of the units is probably beyond the limit of REM.

2.2. Twin boundary and surface reconstruction

As presented in Paper I, {100} twin boundaries were usually observed, but few dislocations were found. Fig. 6 displays two REM images of the surface areas which exhibit twin boundaries as indicated by arrowheads. The surface areas which show the 5×5 reconstruction (in darker contrast) extend across the twin boundaries without being interrupted. There is no indication that the twin boundary nucleates, extends or limits the surface reconstruction, provided one is cautious about the difference in contrast purely introduced by a slight rotation of the twin crystals (i.e. diffraction contrast). Therefore, the formation of the 5×5 reconstruction has no connection with the twin boundaries intersecting the surface.

2.3. Step distribution and surface reconstruction

For semiconductor surfaces, typically the 7×7 surface reconstruction of Si(111) for example, the

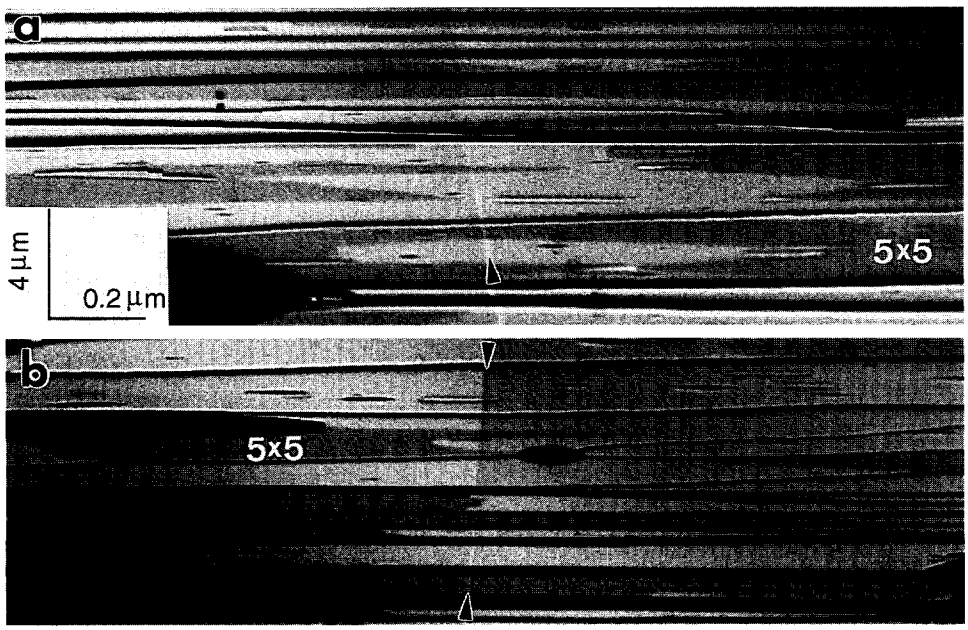

Fig. 6. REM images of the $LaAlO_3(100)$ surface around twin boundaries.

nucleation of the reconstruction is directly associated with the surface steps [5]. It is thus necessary to examine the relationship between the 5×5 reconstruction and the distribution of surface steps. [001] and [010] faceted surface steps are frequently observed on the (100) surface of $LaAlO_3$. In the REM image shown in Fig. 7a, the reconstructed and unreconstructed surface areas are seen and show distinct contrast. Some of the reconstructed areas extend across the step without being interrupted. On some of the surface terraces, both the reconstructed and unreconstructed surface areas co-exist and there is no step to isolate them. In most cases, the reconstructed and non-reconstructed surface areas are not separated

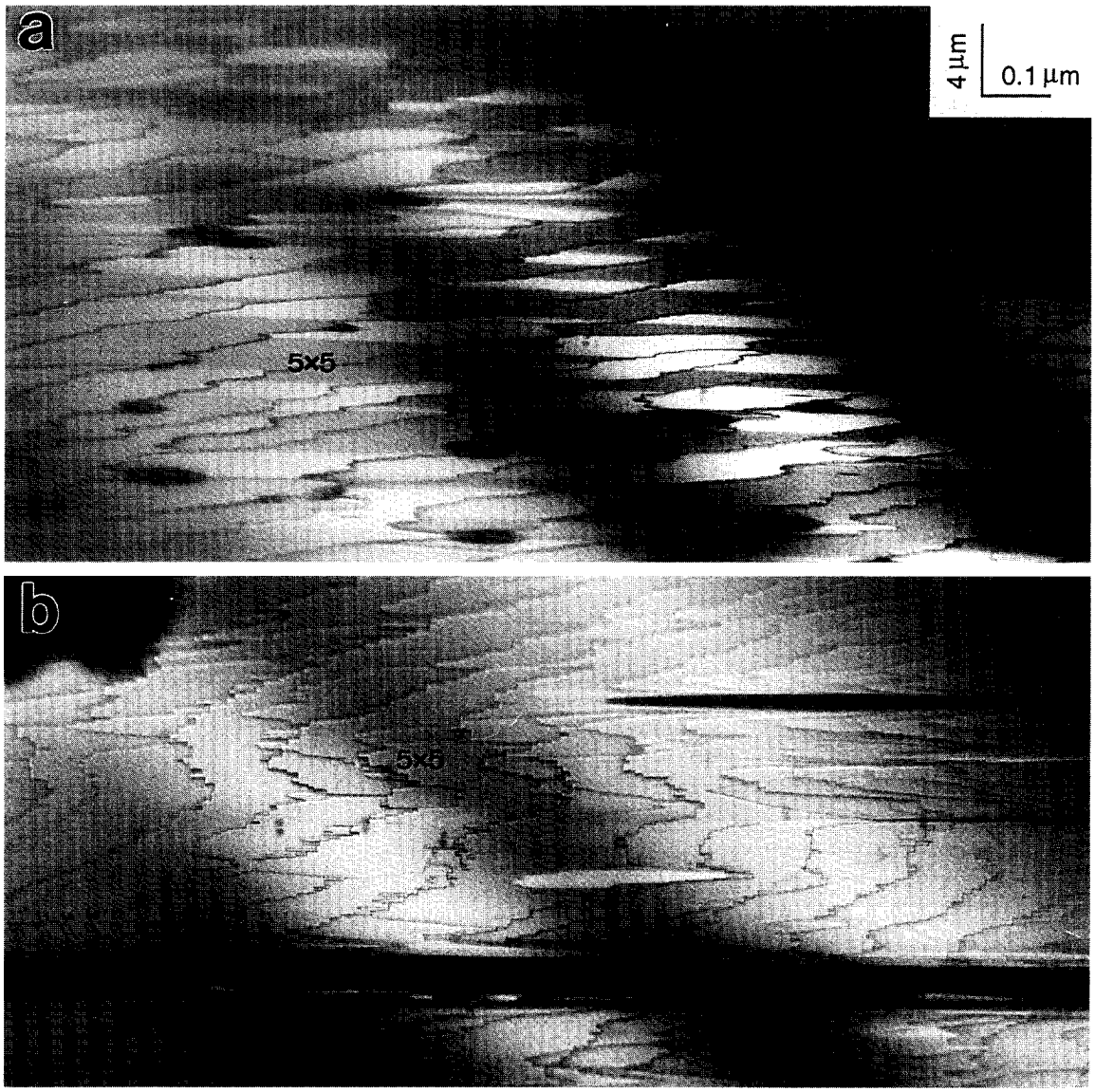

Fig. 7. REM images of the $LaAlO_3(100)$ surface, recorded under the diffracting conditions shown in Fig. 1a, showing the distribution of the reconstructed surface areas. Beam azimuth [001].

by steps. In Fig. 7b, many [001] and [010] steps are seen and the entire surface is almost covered by the reconstructed layer.

Fig. 8a shows a REM image which exhibits many steps. The surface areas with many densely distributed steps are almost entirely covered by the reconstructed layer. The flat areas, as seen on the left- and right-hand sides, are partially covered by the reconstructed layer. It is noticed that the boundaries between the reconstructed and unreconstructed surface regions tend to be parallel to [010]. A few Si–La–O particles are also seen, but there is no association between the surface contaminants and the formation of the reconstruction. This point is clearly seen in Fig. 8b, which displays a REM image recorded from a surface area without any Si–La–O particles. The surface is almost completely covered by the reconstruction layer, especially near the areas with densely distributed steps.

Large plateaus can be formed on the (100) surface. Figs. 9a and 9b show REM images recorded from the left- and right-hand side, respectively, of a plateau region. The plateau is flat and displays 5×5 reconstruction. The surrounding area of the plateau shows many steps, the distribution of which is similar to the distribution of "tiles on a roof". Almost all the steps are along [001] and [010]. Most of the "tiles" are covered by the 5×5 reconstruction. Only a few foreign fragments stand on the surface. In Fig. 9a, the unreconstructed area is more pronounced at the edge of the plateau (see the bright contrast area).

As a summary, the 5×5 reconstruction is observed. The twin boundaries and surface contaminants have little influence on the formation of the reconstruction. The surface steps can enhance the surface reconstruction but are not essential to initiate the reconstruction. This can be explained as follows.

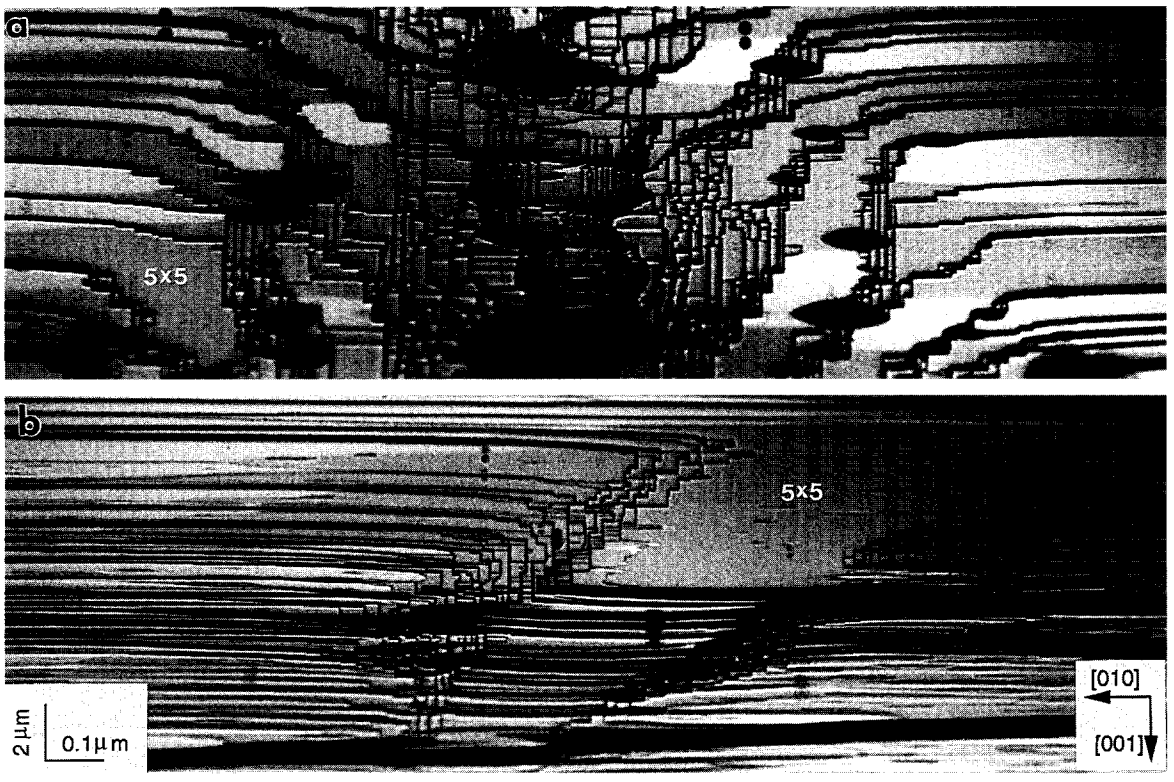

Fig. 8. REM images of the $LaAlO_3(100)$ surface, recorded under the diffracting conditions given by Fig. 1a, showing the distribution of the reconstructed surface areas in the regions where there are many surface steps. Beam azimuth [001].

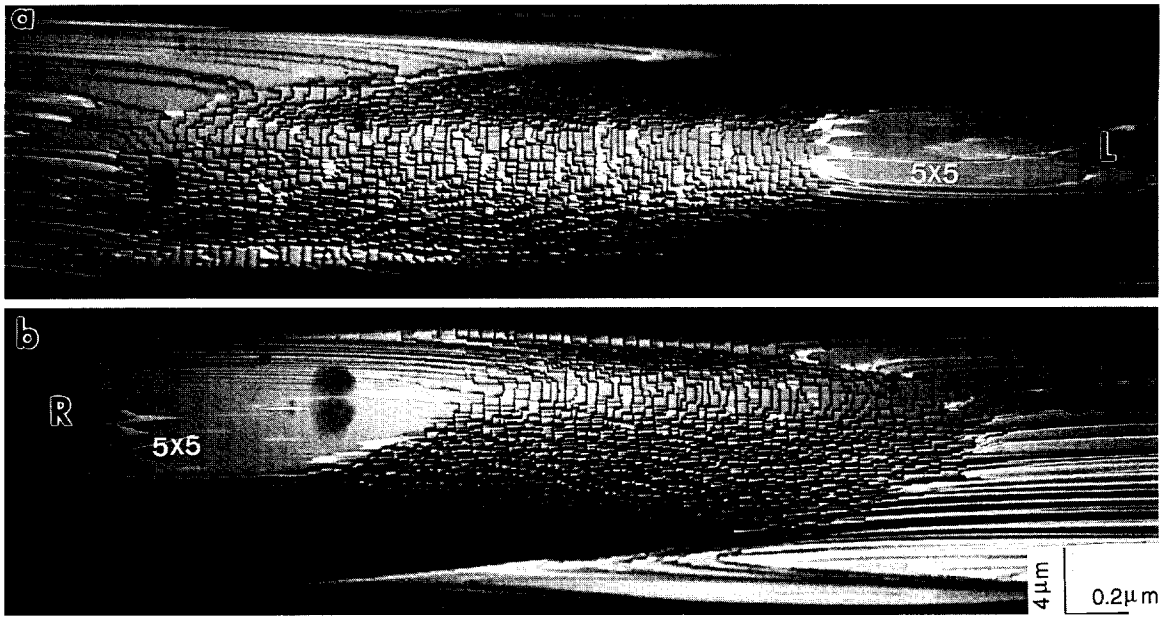

Fig. 9. REM images of the (a) left- and (b) right-hand sides of a plateau area on the $LaAlO_3(100)$ surface. Many [001] and [010] steps are seen, and the surface exhibits the "tiles on a roof" structure. Beam azimuth [001].

In Paper I, we have found that the $LaAlO_3(100)$ surface can be terminated entirely with either the La–O layer or the Al–O layer, but not the mixture of the two. This result is schematically shown in Fig. 10, where, for simplification, only the atoms on the top surface layer are shown. For ionic oxides, the force acting on the surface atoms can be qualitatively determined from the charges of neighboring atoms and their structure symmetries. Since the specimen was annealed in air, it is very possible to have surface adsorption of oxygen. Based on the structure symmetry and the charge distribution near the steps,

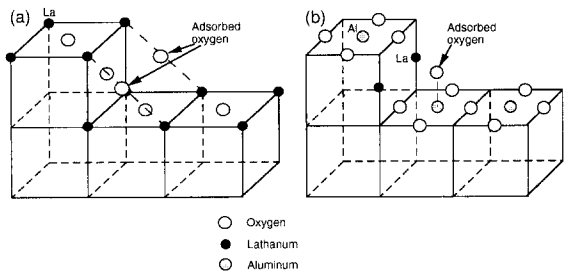

Fig. 10. Schematic models showing the adsorption of oxygen on the surface steps if the surface termination is (a) La–O or (b) Al–O.

the possible models for oxygen adsorption on the steps are shown in Figs. 10a and 10b. One adsorbed oxygen atom is associated with a La or Al atom (note the two adsorbed oxygen atoms shown in Fig. 10a are shared by two unit cells). These models preserve not only the structure symmetry but also the valence states of La and Al. For the La–O terminated surface (Fig. 10a), one oxygen atom is adsorbed per unit step length. Thus the ionic electrostatic force (or bonds) on the La atom located at the step edge is close to being balanced in the plane parallel to the surface. Thus the positions of the La atoms may not change at least in the direction parallel to the (100) plane. If the surface is terminated with the Al–O layer (Fig. 10b), one oxygen atom is adsorbed per unit step length, and the adsorbed oxygen stands on the Al atom. The oxygen adsorption on the step formed by the Al–O terminated terraces is different from that formed by La–O terminated terraces because Al and La have non-equivalent oxygen distributions in $LaAlO_3$. In this configuration, the electrostatic force on the La atom located on the step is almost balanced. Thus they may not be active to initiate the surface reconstruction. Based on these models, surface reconstruction is unlikely to be

directly initiated from the surface step, in agreement with the experimental observations.

Finally, it must be pointed out that the 5×5 reconstruction remained on the surface even after the specimen was exposed to air at room temperature for more than a month. Thus the reconstruction reported here is a stable structure of the surface.

Numerous reconstructions have been observed on surfaces of ionic oxides. A $(\sqrt{3} \times \sqrt{3})$R30° reconstruction has been reported on the NiO(111) surface [6] and the annealed MgO(111) surface [7]. The annealed α-Al_2O_3 $(1\bar{1}02)$ and $(1\bar{1}00)$ surfaces have been found to show reconstructions [8,9]. Reconstruction can also be initiated when the $TiO_2(001)$ surface is contaminated by α-Al_2O_3 during an annealing experiment [10]. A $(\sqrt{5} \times \sqrt{5})$R26.6° reconstruction on reduced $SrTiO_3(100)$ has been observed [11]. However, determining the nature of these surface reconstructions is probably beyond the limit of RHEED and REM.

3. Conclusion

For the first time, 5×5 reconstruction on annealed $LaAlO_3\{100\}$ surfaces is observed with reflection high-energy electron diffraction (RHEED) and reflection electron microscopy (REM). Most of the {100} surfaces were covered by the reconstructed layer. It is suggested from RHEED observation that the reconstructed supercell may be composed of two types of structural units which have different structures. The presence of twin boundaries and Si–La–O contaminants on the surface have little influence on the formation of surface reconstruction. The [001] and [010] surface steps may enhance the reconstruction but are not essential to initiate the reconstruction. The non-catalytic effect of surface steps in producing the reconstruction is interpreted based on the adsorption models of oxygen on surface steps.

References

[1] Z.L. Wang and A.J. Shapiro, Surf. Sci. 328 (1995) 141.
[2] S. Geller and V.B. Bala, Acta Cryst. 9 (1956) 1019.
[3] G.W. Berkstresser, A.J. Valentino and C.D. Brandle, J. Cryst. Growth 109 (1991) 467.
[4] Z.L. Wang, J. Bentley, E.A. Kenik, L.L. Horton and R.A. McKee, Surf. Sci. 273 (1992) 88.
[5] A.V. Latyshev, A.B. Krasilnikov, L.V. Sokolov and S.I. Stenin, Surf. Sci. 254 (1991) 90.
[6] N. Floquet and L.-C. Dufour, Surf. Sci. 126 (1983) 543.
[7] M. Gajdardziska-Josifovska, P.A. Crozier and J.M. Cowley, Surf. Sci. 248 (1991) L259.
[8] T. Hsu and Y. Kim, Surf. Sci. 258 (1991) 119.
[9] J. Liu and J.M. Cowley, Proc. 49th Annu. Meeting. of Electron Microsc. Soc. of America, Ed. G.W. Bailey (San Francisco Press, San Francisco, CA, 1991) p. 630.
[10] J. Liu, L. Wang and J.M. Cowley, Surf. Sci. 268 (1992) L293.
[11] T. Matsumoto, H. Tanaka, K. Kouguchi, T. Kawai and S. Kawai, Surf. Sci. 312 (1994) 21.